Analysis of the Raman spectral shape in α-AgI

E. Cazzanelli, A. Fontana, and G. Mariotto
Department of Physics, University of Trento, I-38050 Povo (Trento), Italy
and Gruppo Nazionale di Struttura della Materia, Consiglio Nazionale delle Ricerche, I-38050 Povo (Trento), Italy

V. Mazzacurati, G. Ruocco, and G. Signorelli
Department of Physics, University "La Sapienza," Piazzale Aldo Moro 2, I-00185 Roma, Italy
and Gruppo Nazionale di Struttura della Materia, Consiglio Nazionale delle Ricerche, I-00185 Roma, Italy
(Received 17 January 1983; revised manuscript received 13 June 1983)

In this paper we present a detailed analysis of the Raman spectral shape of α-AgI crystals as a function of temperature up to 450 °C. With the use of a polarizability model based on the charge-induced dipole mechanism, which was already introduced to explain depolarization ratios and integrated intensities, all the spectral features from 0.8 to 250 cm^{-1} are assigned to the iodine dynamics (acoustical and optical phonons), in agreement with inelastic-neutron-scattering data. Hence we predict that the central line originating from Ag^+ diffusive motions must be confined to the frequency region below 0.8 cm^{-1}. Some suggestions on the phonon branches are qualitatively derived from the temperature dependence of the spectral shape.

I. INTRODUCTION

The experimental data already reported[1,2] on the Raman spectrum of α-AgI in the frequency range 7—165 cm^{-1} show that both the integrated Raman spectral density and the depolarization ratio (which was also found to be constant versus frequency) were strongly temperature dependent, decreasing up to 450 °C.

In order to explain this unusual behavior we proposed in a previous paper,[3] hereafter referred to as I, a model, in which all the observed light scattering is explained by a simplified charge-induced dipole (CID) mechanism. In such a way we were able to relate the two measured quantities with the arrangement of the mobile cations in the possible sites. The observed temperature behavior of depolarization ratio and integrated intensity were theoretically accounted for by introducing a correlation in the spatial distribution of the silver ions, which was destroyed by increasing temperature. Nevertheless, no attempt was made in I to analyze the spectral shape, which was tentatively attributed to vibrational dynamics of the iodine atoms. Different interpretations of this spectrum have been already given in the literature. Its broad, smooth, and structureless shape first suggested to Delaney and Ushioda[4] an explanation in terms of two-phonon scattering. From the similarity between the spectra in α and β phases near the transition temperature, the reduced spectral density was qualitatively assigned to the one-phonon density of states[5] induced in the first-order Raman scattering by the presence of the disordered Ag^+ sublattice. Alben *et al.*[6] reached the same conclusion by means of a modified latttice-dynamics calculation, taking into account the neutron scattering results from Bührer *et al.*[7] On the contrary, Winterlingh *et al.*[8] tried to decompose the spectrum below 50 cm^{-1} into two different components, both related to the motion of the silver ions: they suggest that the narrow one is due to the silver jump diffusion and the broader one to its random local motion in each quasiequilibrium site. The same kind of analysis had also been adopted by Nemanich *et al.*[9] on the basis of very similar experimental data. In the Winterlingh and Nemanich works, however, no interest was devoted to the high-frequency part of the spectrum (which is well above the Ag^+ dynamical range) and to the temperature dependence of both the intensity and depolarization ratio.

In order to clarify this problem, our theoretical procedure will be adopted in calculating the entire spectral shape down to the lower observed frequency limit, as well as the depolarization ratios and integrated intensities of the different scattering contributions. The theoretical results will be then compared with the available experimental data. Our previous measurements have been also extended to the frequency region 2—250 cm^{-1} for all temperatures, with increased accuracy and resolution, mainly in the low-frequency part (2—30 cm^{-1}). We anticipate that these spectra are identical to the ones reported by Winterlingh, so that our conclusions may be extrapolated with good confidence down to their lower-frequency limit (0.8 cm^{-1}).

II. DISORDER-INDUCED RAMAN SPECTRUM

On the basis of simple physical considerations we have already assumed that the entire depolarized Raman spectrum in α-AgI is due to the disordered anisotropic polarizability induced on each ion by the local electric field of the surrounding Ag^+ charges.

Indeed, thanks to the cubic symmetry of the iodine sublattice, their contribution to the local field cannot be present on either iodine or silver ions (which we suppose localized in their quasiequilibrium positions). The relative motion of the ions will give rise to fluctuations in the lo-

cal electric fields: then the Ag^+ dynamics will appear in both Ag^+-Ag^+ and Ag^+-I^- contributions to the scattering, while I^- dynamics will be reflected only in the second-order contribution. Now the macroscopic polarizability $P_{\gamma\gamma'}(\vec{r},t)$ ($\gamma\gamma'=x,y,z$) may be written as

$$P_{\gamma\gamma'}(\vec{r},t)=\sum_{i,l} p^{il}_{\gamma\gamma'}(t)\delta(\vec{r}-\vec{R}_{il}(t)) + \sum_{a} p^{a}_{\gamma\gamma'}(t)\delta(\vec{r}-\vec{R}_{a}(t)) , \quad (1)$$

where l is the cell index, $i=1,2$ indicates the iodine in the primitive cell, and $a=1,\ldots,N$ refers to all the silver ions.

The integrated contribution of the iodine dynamics to the scattered intensity was already evaluated as

$$^1I_{\gamma\gamma'}(T)=J_{\gamma\gamma'}(T)\langle u^2\rangle , \quad (2)$$

where $J_{\gamma\gamma'}(T)$ is defined in Eqs. (3), (5), and (10) of I, and $\langle u^2\rangle$ represents the mean-square displacements of the iodine nuclei. With the same procedure we may now calculate the integrated scattering intensity related to the silver dynamics in the first term on the right-hand side of Eq. (1) as

$$^2I_{\gamma\gamma'}(T)=p^2\sum_{n,k} W(C_{nk},T)\mathscr{E}^4_{nk}\langle f^2_{\gamma\gamma'}\rangle_{C_{nk}} . \quad (3)$$

In Eq. (3) we retain the same definitions of I.

A rough evaluation of the ratio between these two terms is given for the zz configuration and in the low-temperature region by

$$\frac{^1I_{zz}}{^2I_{zz}}=2\times10^2\frac{q_p^*\langle u^2\rangle}{\mathscr{E}^2_{3,0}D^6}\sim2\times10^2\frac{\langle u^2\rangle}{D^2} , \quad (4)$$

where D is the distance between an iodine and the surrounding d sites. It may be observed that, while the integrated intensities of these two contributions are of the same order of magnitude, their ratio must be a linear function of the temperature because of the temperature dependence of $\langle u^2\rangle$. Moreover, the depolarization ratio of the silver contribution is strongly different from that of the iodine contribution, which agrees with the experimental value and behaves also differently with temperature. We write

$$^2R(180\,^\circ\mathrm{C})=\frac{^2I_{xz}(180\,^\circ\mathrm{C})}{^2I_{zz}(180\,^\circ\mathrm{C})}=0 ,$$

$$^1R(180\,^\circ\mathrm{C})=\frac{^1I_{xz}(180\,^\circ\mathrm{C})}{^1I_{zz}(180\,^\circ\mathrm{C})}=1.05\simeq R_{\mathrm{obs}} ,$$

$$^2R(450\,^\circ\mathrm{C})=\frac{^2I_{xz}(450\,^\circ\mathrm{C})}{^2I_{zz}(450\,^\circ\mathrm{C})}=1.5 ,$$

$$^1R(450\,^\circ\mathrm{C})=\frac{^1I_{xz}(450\,^\circ\mathrm{C})}{^1I_{zz}(450\,^\circ\mathrm{C})}=0.69\simeq R_{\mathrm{obs}} .$$

If the $^2I_{\gamma\gamma'}(\omega)$ contribution is in some way superimposed to the iodine vibrational density of states, $^1I_{\gamma\gamma'}(\omega)$, then the depolarization ratio measured would be frequency dependent and the spectral shape would change drastically with temperature.

Because these conclusions are contrary to all the reported experimental results, we must conclude that the spectral range of the $^2I_{\gamma\gamma'}(\omega)$ contribution must be narrower than 2 cm^{-1}.

As far as the scattering arising from $p^a_{\gamma\gamma'}(t)$ term in Eq. (1), it is easy to show that its spectral shape has to be the same of $^2I_{\gamma\gamma'}(\omega)$ in the limit of very small exchanged wave vectors. Therefore the same conclusion derived for $^2I(\omega)$ also holds for this term, definitively excluding that any observed features of the spectra above 2 cm^{-1} may be connected with the Ag^+ dynamics.

In the next section we try to calculate the spectral shape arising from the iodine dynamics in order to compare the theoretical prediction with the experimental data.

III. SPECTRAL SHAPE OF ONE-PHONON SCATTERING IN α-AgI

In order to calculate the spectral response we are interested in, we have to deal now just with the scattering contribution $^1I_{\gamma\gamma'}$. If we suppose that Ag^+ motions to be uncorrelated from the iodine vibrations, the leading one-phonon scattering term could be written as

$$I_{\gamma\gamma'}(\omega)\propto\sum_{\substack{i,l,\\ i',l'}} e^{-i\vec{q}\cdot(\vec{x}_{il}-\vec{x}_{i'l'})}\int dt\, e^{i\omega t}\sum_{\alpha,\beta}[\langle {}^{\alpha}v^{il}_{\gamma\gamma'}(t)\,{}^{\beta}v^{i'l'}_{\gamma\gamma'}(0)\rangle]_{\mathrm{av}}\langle u^{\alpha}_{il}(t)u^{\beta}_{i'l'}(0)\rangle , \quad (5)$$

where $\langle\ \rangle$ and $[\ ]_{\mathrm{av}}$ indicate, respectively, thermal and configurational averages. Using the approximation $\vec{q}\cdot(\vec{x}_{il}-\vec{x}_{i'l'})\simeq\vec{q}\cdot(\vec{x}_l-\vec{x}_{l'})$, the normal-modes expansion of the atomic displacements and the convolution theorem, we obtain, from Eq. (5),

$$I_{\gamma\gamma'}(\omega)\propto\sum_{\vec{k},j}\omega_j(\vec{k})\sum_{l,l'}e^{-i(\vec{q}-\vec{k})\cdot(\vec{x}_l-\vec{x}_{l'})}\sum_{\substack{\alpha,\beta\\ i,i'}}e^{\alpha}(\vec{k},j\mid i)e^{\beta}(\vec{k},j\mid i')\int d\omega' F^{\gamma\gamma'}_{\alpha\beta}(i,i';l,l';\omega-\omega')[n(\omega')+1]\mathrm{Im}\,D_{\vec{k}j}(\omega') ,$$

(6)

where

$$F^{\gamma\gamma'}_{\alpha\beta}(i,i';l,l';\omega)=\int dt\, e^{i\omega t}[\langle {}^{\alpha}v^{il}_{\gamma\gamma'}(t)\,{}^{\beta}v^{i'l'}_{\gamma\gamma'}(0)\rangle]_{\rm av}$$
$$=\int dt\, e^{i\omega t}\tilde{F}^{\gamma\gamma'}_{\alpha\beta}(i,i';l,l';t)\ .$$

j is the branch index, $\vec{k}$ is the phonon wave vector, and $\omega_j(\vec{k})$ and $\vec{e}(\vec{k},j\mid i)$ are, respectively, its eigenfrequency and eigenvector. $D_{\vec{k}j}(\omega)$ is the phonon propagator, which, in the harmonic approximation reduces to

$$D_{\vec{k}j}(\omega)=\lim_{\epsilon\to 0^+}2\omega_j(\vec{k})/[\omega^2-\omega_j^2(\vec{k})+2i\omega\epsilon]\equiv D^0_{\vec{k}j}(\omega)\ . \tag{7}$$

Owing to the slow motion of the Ag^+ ions, we may write, in this case,

$$F^{\gamma\gamma'}_{\alpha\beta}(i,i';l,l';\omega)=\delta(\omega)\tilde{F}^{\gamma\gamma'}_{\alpha\beta}(i,i';l,l';t=0)\ . \tag{8}$$

$F^{\gamma\gamma'}_{\alpha\beta}$ is connected with the quantity $J_{\gamma\gamma'}$ already introduced in I by the relation

$$J_{\gamma\gamma'}=\sum_{i,l}\sum_{\alpha,\beta}\tilde{F}^{\gamma\gamma'}_{\alpha\beta}(i,i;l,l;t=0)\ . \tag{9}$$

In I we treated the scattering equation assuming no correlation between the local electric field on two different iodines; on the other hand, in order to calculate the frequency dependence of the scattering intensity, we need go beyond this approximation.

In Appendix A we show, by introducing a model correlation function between different scatterers and making use of Eq. (8), that Eq. (6) becomes

$$I_{\gamma\gamma'}(\omega)\propto[n(\omega)+1]\times\sum_{\vec{k},j}\frac{e^{-|\vec{k}-\vec{q}|^2/2\bar{K}^2}}{\bar{K}^3}\,{\rm Im}\,D_{\vec{k}j}(\omega)/\omega_j(\vec{k})J_{\gamma\gamma'}\ , \tag{10}$$

where $\vec{k}$ is a wave vector related to the typical correlation length of the polarizability derivatives. This quite general expression shows the effect of the polarizability disorder on the Raman spectrum. Actually, full disorder in the scattering amplitudes implies $\bar{K}$ greater than the Brillouin-zone edge $\vec{K}_B$ and allows all the $(\vec{k},j)$ modes to participate to the scattering process; hence in the harmonic approximation, the intensity $I_{\gamma\gamma'}(\omega)$ may be written as

$$I_{\gamma\gamma'}(\omega)\propto[n(\omega)+1]\rho(\omega)/\omega\ . \tag{11}$$

In ordered crystals, on the other hand, $\vec{k}\to 0$, and

$$I_{\gamma\gamma'}(\omega)\propto[n(\omega)+1]\sum_j C^{\vec{q}}_{\gamma\gamma'}\delta(\omega-\omega_j(\vec{q}))/\omega\ , \tag{12}$$

giving rise to narrow peaks in the spectrum, which are the Raman-active phonons for $\vec{k}=\vec{q}\simeq 0$.

The partial disorder may be taken into account by a finite value of $\bar{K}$, and with $|\vec{q}|\ll|\vec{k}|$, Eq. (10) can be written in the simple form

$$I_{\gamma\gamma'}(\omega)\propto[n(\omega)+1]J_{\gamma\gamma'}\sum_{\vec{k},j}\frac{e^{-k^2/2\bar{K}^2}}{\bar{K}^3}\,{\rm Im}\,D_{\vec{k}j}/\omega_j(\vec{k})\ . \tag{13}$$

IV. COMPARISON BETWEEN THEORY AND EXPERIMENTAL RESULTS

In order to obtain the Raman spectral shape by means of Eq. (13) we need the phonon dispersion relations, a value for the parameter $\bar{K}$ and an adequate choice for the propagator $D_{\vec{k}j}(\omega)$. Inelastic-neutron-scattering data[10] are available at $T=300\,^{\circ}$C up to 40 cm^{-1}: In this frequency range all the excitations of the crystal are shown to be transverse- and longitudinal-acoustical (TA and LA) waves. We conclude that the optical-mode contribution could be present only above this frequency and then we will try to fit the spectrum for $\omega\le 40$ cm^{-1} using only the acoustical (acous) contribution,

$$I_{\gamma\gamma'}(\omega)\simeq I^{\rm acous}_{\gamma\gamma'}(\omega)=I^{\rm LA}_{\gamma\gamma'}(\omega)+I^{\rm TA}_{\gamma\gamma'}(\omega),\quad \omega\le 40\ {\rm cm}^{-1}\ . \tag{14}$$

Neutron data indicate that a linear dispersion relation and harmonic propagators can be adopted for the longitudinal branch at all $\vec{k}$ values up to $\bar{K}$ which we approximately evaluate as 0.25 Å^{-1} (see Appendix A). Hence,

$$I^{\rm LA}_{\gamma\gamma'}\propto G^{\rm LA}J_{\gamma\gamma'}[n(\omega)+1]\omega\frac{1}{\bar{K}^3}e^{-\omega^2/2C_L^2\bar{K}^2}\ , \tag{15}$$

where $G^{\rm LA}=\Omega/\pi^2C_L^2$ and Ω is the volume of the sample.

The same experimental data show the TA branch to be strongly anharmonic; the simplest choice for $D^{\rm TA}_{\vec{k}j}(\omega)$ can be given by the overdamped classical oscillator response function[11]

$$D^{\rm TA}_{\vec{k}j}(\omega)=2\omega_{\rm TA}(\vec{k})D_{\rm TA}/[\omega^2-\omega^2_{\rm TA}(\vec{k})+i\omega\Gamma_{\rm TA}(\vec{k})]\ , \tag{16}$$

where $\omega_{\rm TA}(\vec{k})$ and $\Gamma_{\rm TA}(\vec{k})$ are derived from the reported neutron data, and $D_{\rm TA}$ represents an adimensional oscillator strength. We assume $D_{\rm TA}$ to be $\vec{k}$ independent because the ratio $\Gamma_{\rm TA}(\vec{k})/\omega_{\rm TA}(\vec{k})$ is constant versus $\vec{k}$ up to $\bar{K}$.

The transverse contribution can be therefore explicitly calculated,

$$I^{\rm TA}_{\gamma\gamma'}(\omega)\propto G^{\rm TA}J_{\gamma\gamma'}[n(\omega)+1]\omega\mathcal{F}(\omega,\bar{K})\ , \tag{17}$$

with $G^{\rm TA}=2\Omega D_{\rm TA}/\pi^2C_T^3$, and

$$\mathcal{F}(\omega,\bar{K})=C_T^3\int_0^{K_B}dk\,k^2e^{-k^2/2\bar{K}^2}\Gamma_{\rm TA}(\vec{k})/\{[(\omega^2-\omega^2_{\rm TA}(\vec{k})]^2+\omega^2\Gamma_{\rm TA}(\vec{k})\}\ . \tag{18}$$

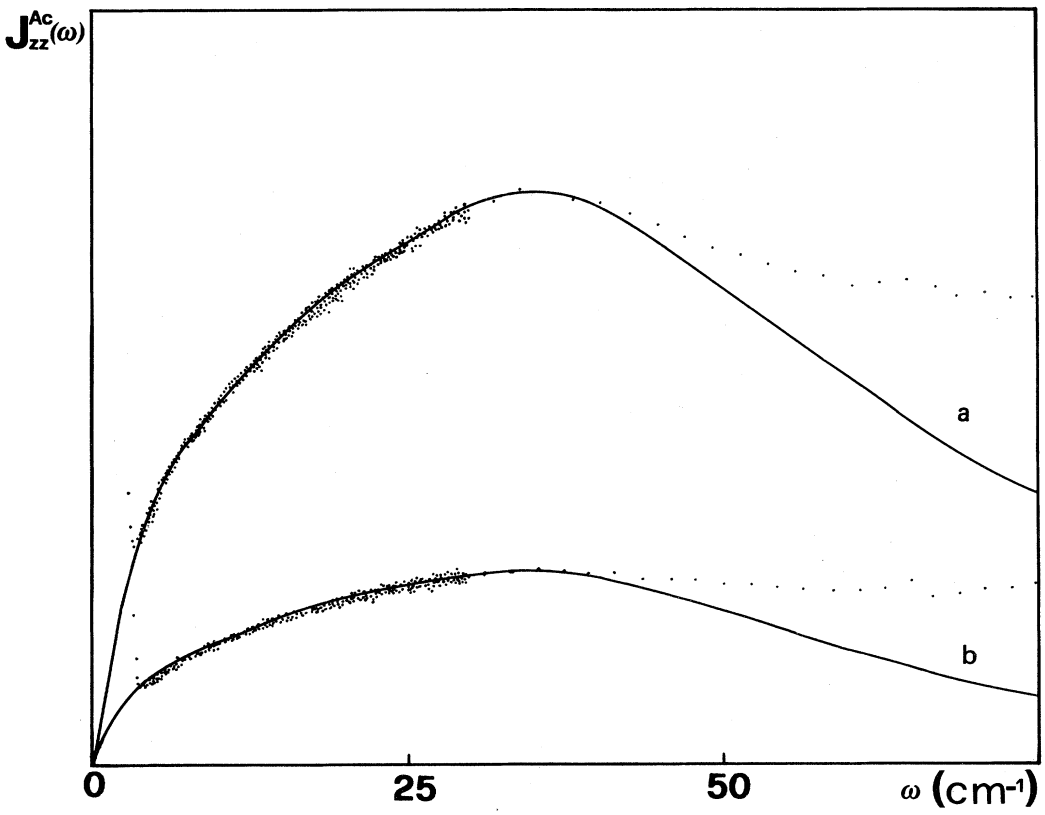

FIG. 1. Solid dots denote experimental Raman scattering normalized by the appropriate Bose-Einstein population factor $n(\omega,T)+1$. From 2 to 30 cm^{-1} the spectral resolution was 0.2 cm^{-1}, and above 30 cm^{-1} it was 2 cm^{-1}. Solid line plots the acoustical spectral density as obtained by Eq. (19): *a* at $T=300\,°C$ and *b* at $T=380\,°C$.

The whole acoustical reduced spectral density can now be written as

$$J_{\gamma\gamma'}^{\text{acous}}(\omega)=\frac{I_{\gamma\gamma'}^{\text{acous}}(\omega)}{[n(\omega)+1]}\propto J_{\gamma\gamma'}\omega[e^{-\omega^2/2C_L^2\bar{K}^2}+G\mathcal{F}(\omega,\bar{K})]\ , \tag{19}$$

and this expression can be fitted to the experimental spectrum for $\omega\lesssim 40$ cm^{-1} using two parameters: $G=2(C_L/C_T)^3D_{\text{TA}}$, completely free, and $\bar{K}$ limited in the wave-vector interval 0.2–0.3 $Å^{-1}$, in agreement with its estimate carried out in Appendix B.

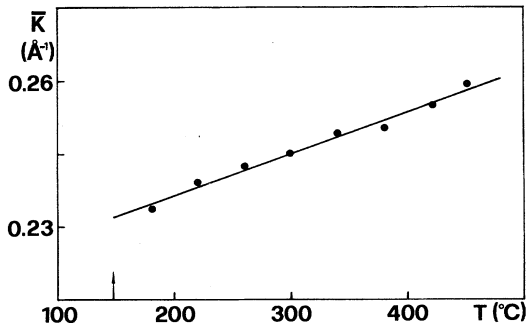

FIG. 2. Temperature dependence of $\bar{K}$ parameters as obtained by the fit of experimental data; solid line is the linear best fit. Arrow indicates the $\beta\rightarrow\alpha$ phase-transition temperature.

In Fig. 1 we report the results of the best fits at two different temperatures. For $T=300\,°C$, $K=0.245$ $Å^{-1}$, and $D_{\text{TA}}=5\times10^{-3}$.

The agreement between theoretical and experimental spectral shapes is excellent in the frequency range 0.8–40 cm^{-1} for all the measured spectra with the same value of G and with $\bar{K}$ slowly increasing versus temperature (see Fig. 2). It can be observed, on the contrary, that the overall spectral density is larger than the one given by Eq. (19) in the region above 40 cm^{-1} where the importance of the contribution of the optical modes has been already recognized.[1] The difference

$$J_{\gamma\gamma'}^{\text{opt}}(\omega)=J_{\gamma\gamma'}^{\text{expt}}(\omega)-J_{\gamma\gamma'}^{\text{acous}}(\omega)\ , \tag{20}$$

which represents the "weighted" optical density of states (see Appendix A), is shown in Fig. 3 for three different temperatures. We may note that its shape is quite temperature independent, while the ratio

$$\chi(T)=\int_0^\infty d\omega J_{\gamma\gamma'}^{\text{opt}}(\omega)\Big/\int_0^\infty d\omega J_{\gamma\gamma'}^{\text{LA}}(\omega) \tag{21}$$

(reported in Fig. 4) is proportional to $\bar{K}$. This result can be theoretically predicted by performing the integral of scattering equation (13) (see Appendix B) by assuming a small $\vec{k}$ dispersion for the optical branches, which is quite a reasonable hypothesis.

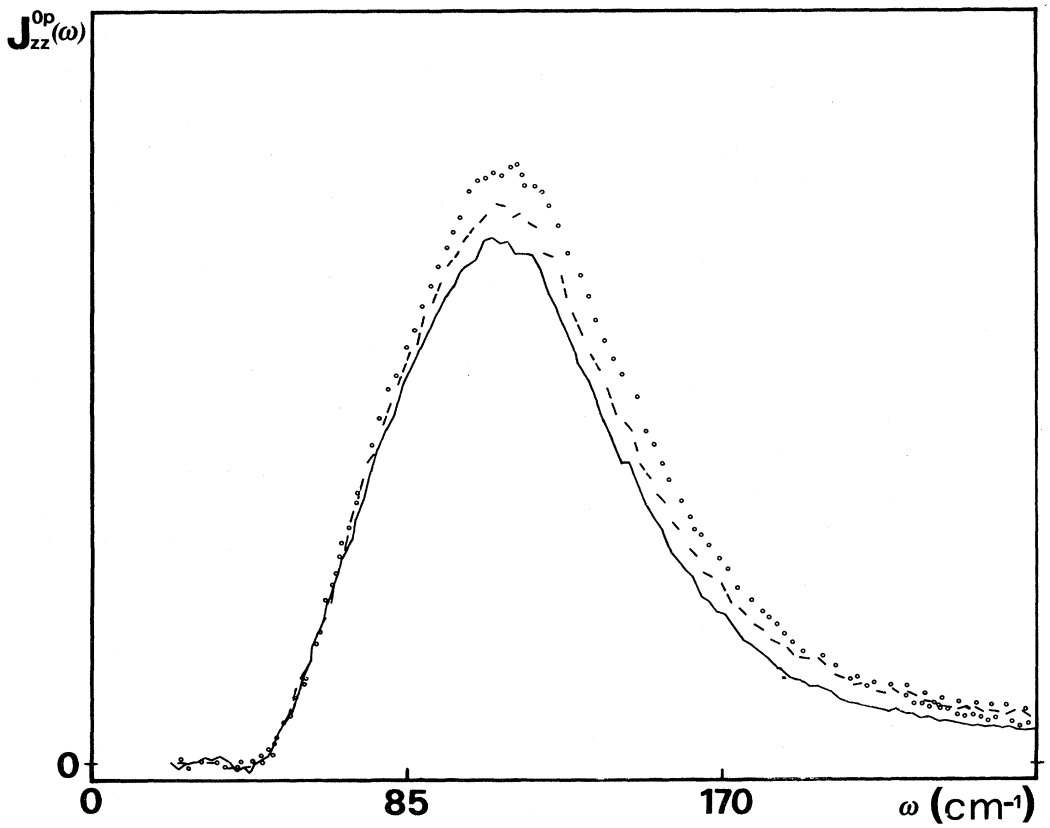

FIG. 3. Optical density of states obtained as described in the text at three significant temperatures: $T=180\,^{\circ}$C (line), 260°C (dashed line), and 340°C (dotted line). This density is peaked about 110 cm^{-1} and its shape is temperature independent.

V. DISCUSSION AND CONCLUSIONS

A detailed analysis of the Raman spectrum of α-AgI crystals has been developed as a function of temperature up to 450°C using the polarizability model already proposed in I. All the spectral features in the (0.8—250)-cm^{-1} region are assigned to the iodine dynamics and are quantitatively accounted for by a weighted density of states of both acoustic and optical phonons. Since we have quantitatively accounted for the spectrum above 0.8 cm^{-1} we assign any central line due to the Ag^+ diffusive motion (whose contribution to the light scattering we evaluate to be of the same order of magnitude as the one relative to iodine) to be limited to the spectral region below 0.8 cm^{-1}. Experiments are in progress in that frequency range to reveal and measure the predicted Ag^+ contribution by means of interferometric techniques.

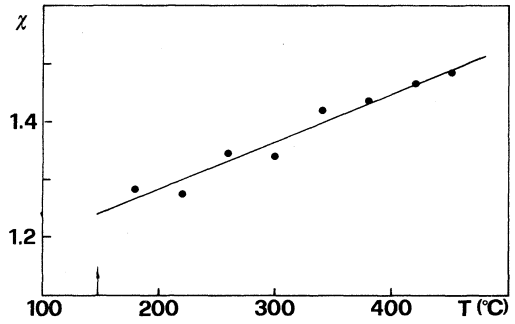

FIG. 4. Plot of the ratio between the integrated intensity of TO and LA phonons as a function of temperature: Best fit indicates linear behavior. Arrow indicates the $\beta \rightarrow \alpha$ phase-transition temperature.

The present data already analyzed allow us to deduce some properties of the iodine motion as well as some properties of the average Ag^+ distribution. We present the following:

(a) The high anharmonicity of the TA branch, already observed by inelastic neutron scattering at $T=300\,^{\circ}$C, is seen from our analysis to be temperature independent. This suggests that the short lifetime of these excitations can be due to their interaction with some relaxation of the "melted" Ag^+ sublattice rather than to phonon-phonon processes. An empirical description of such phenomenon has been already given by Winterling[12] to account for the Brillouin line shape in vitreous silica and was also discussed by Fleury.[13] In these works a lowering in the phonon oscillator strength has been predicted for high values of the relaxation strength g (see Ref. 12, p. 2436), which is in good agreement with the low value of D_{TA} we find in fitting experimental data to Eq. (19).

(b) Clear evidence of the existence of optic modes in

α-phase AgI is obtained in the frequency region 40—250 cm^{-1}, exactly where β-AgI also shows its optical contribution. No other experimental data are available in current literature on such excitations; therefore it may be useful to deduce even qualitatively some of their properties. From the experimental value of the ratio between the integrated intensity of such band and the LA contribution, which is 1.3, we may deduce the presence of three branches of quasiharmonic excitations ($\Gamma_{\vec{k}} < \omega_{\vec{k}}$) having small $\vec{k}$ dispersion at least for $\vec{k} < \bar{K}$ (see Appendix B). The quasiharmonicity of such phonons is also supported by the weak temperature dependence of the line shape, already stressed in Sec. IV.

(c) As far as the Ag^+ arrangement is concerned, the increase of $\bar{K}$ with temperature, obtained by fitting the acoustical contribution, corresponds to a decrease in the correlation length and qualitatively confirms the order-disorder evolution of the system which was already discussed in I. Nevertheless, $\bar{K}$ cannot significantly change because its low-temperature value is already very near to its upper limit established by the Ag^+-Ag^+ repulsion, which excludes the occupation of nearest-neighbor d sites.

APPENDIX A

Using relation (8) we may write the general expression for the one-phonon leading term,

$$I_{\gamma\gamma'}(\omega) \propto \sum_{\vec{k},j} \frac{1}{2\omega_j(\vec{k})} \Theta^{\gamma\gamma'}(\vec{k},j \mid \vec{q}) \mathrm{Im}\, D_{\vec{k}j}(\omega) , \tag{A1}$$

where the weighting factor $\Theta^{\gamma\gamma'}(\vec{k},j \mid \vec{q})$ is given by

$$\Theta^{\gamma\gamma'}(\vec{k},j \mid \vec{q}) = \sum_{l,l'} e^{-i(\vec{q}-\vec{k})\cdot(\vec{x}_l - \vec{x}_{l'})} \sum_{i,i'} (M_i M_{i'})^{-1/2} e^{-i\vec{q}\cdot(\vec{X}_i - \vec{X}_{i'})} \sum_{\alpha,\beta} \tilde{F}^{\gamma\gamma'}_{\alpha\beta}(i,i';l,l';t=0) e^{\alpha}(\vec{k},j \mid i) l^{*\beta}(\vec{k},j \mid i) , \tag{A2}$$

and the quantity $\tilde{F}^{\gamma\gamma'}_{\alpha\beta}(i,i';l,l';t=0)$ represents the configurational average of the polarizability derivatives, i.e.,

$$\tilde{F}^{\gamma\gamma'}_{\alpha\beta}(i,i';l,l';t=0) = {}^{\alpha}v^{il}_{\gamma\gamma'} {}^{\beta}v^{i'l'}_{\gamma\gamma'}, \quad {}^{\alpha}v^{il}_{\gamma\gamma'} = \sum_{a} \frac{\partial P^{il}_{\gamma\gamma'}}{\partial X^{\alpha}_{ila}} , \tag{A3}$$

which was already calculated in I for $i=i', l=l'$ [here used in Eq. (9)]. An important property of $\tilde{F}^{\gamma\gamma'}_{\alpha\beta}(i,i';l,l';t=0)$ in the case of CID scattering in α-AgI is

$$\tilde{F}^{\gamma\gamma'}_{\alpha\beta}(i,i';l,l';t=0) = \delta_{\alpha\beta} \tilde{F}^{\gamma\gamma'}_{\alpha\alpha}(i,i';l,l';t=0) = \delta_{\alpha\beta} \tilde{F}^{\gamma\gamma'}(i,i';l,l';t=0) . \tag{A4}$$

In order to prove relation (A4) we note from Eq. (9′) in I that the polarizability derivative ${}^{\alpha}v^{il}_{\gamma\gamma'}$ depends on the direction of the electric field $\vec{\mathscr{E}}_{il}$ created on the (i,l) iodine by the silver ions belonging to its d-site environment (cage): for example ${}^{\alpha}v^{il}_{\gamma\gamma'} = {}^{\alpha}v_{\gamma\gamma'}(\vec{\Omega}_{il})$ where $\vec{\Omega}_{il}$ indicates the Eulerian angles of the field $\vec{\Omega}_{il} \equiv (\theta_{il}, \varphi_{il})$. Because of the high number of possible arrangements of the silver ions in the cage (already discussed in I) many directions are allowed for $\vec{\mathscr{E}}_{il}$. We may introduce a probability function $\Pi^{il}(\vec{\Omega}) d\vec{\Omega}$ for the field to be directed along $\vec{\Omega}$ into the solid angle $d\vec{\Omega}$: Then the configurational average for $i=i'$ and $l=l'$ can be performed by an integration

$$\tilde{F}^{\gamma\gamma'}_{\alpha\beta}(i,i';l,l;t=0) = \int d\vec{\Omega}\, \Pi^{il}(\vec{\Omega}) {}^{\alpha}v_{\gamma\gamma'}(\vec{\Omega}) {}^{\beta}v_{\gamma\gamma'}(\vec{\Omega}) . \tag{A5}$$

We need to generalize this expression for $i \neq i'$ and $l \neq l'$, keeping in mind that a given field direction on iodine (il) excludes a number of possible directions for the field on its neighboring iodines, giving, in such a way, a correlation between the directions of the fields on different iodines. Therefore, we may introduce a conditioned probability function $\Pi^{ili'l'}(\vec{\Omega}_1, \vec{\Omega}_0) d\vec{\Omega}_1$ in terms of which $\tilde{F}^{\gamma\gamma'}_{\alpha\beta}(i,i';l,l';t=0)$ may be calculated, assuming that $\Pi^{ilil}(\vec{\Omega}_1, \vec{\Omega}_0) = \delta(\vec{\Omega}_1 \cdot \vec{\Omega}_0)$. In the general case, we may write

$$F^{\gamma\gamma'}_{\alpha\beta}(i,i';l,l';t=0) = \int d\vec{\Omega}_0 \int d\vec{\Omega}_1 \Pi^{il}(\vec{\Omega}_0) \Pi^{ili'l'}(\vec{\Omega}_1, \vec{\Omega}_0) {}^{\alpha}v_{\gamma\gamma'}(\vec{\Omega}_0) {}^{\beta}v_{\gamma\gamma'}(\vec{\Omega}_1) . \tag{A6}$$

Through Eq. (9′) in I we may derive an expression of ${}^{\alpha}v^{il}_{\gamma\gamma'}$ in terms of Cartesian components,

$$\vec{r}_{il} \equiv (r^{\alpha}_{il}) \equiv (x_{il} = \sin\theta_{il}\cos\varphi_{il}, y_{il} = \sin\theta_{il}\sin\varphi_{il}, z_{il} = \cos\theta_{il}) ,$$

$${}^{\alpha}v_{\gamma\gamma'}(\vec{\Omega}_{il}) = \xi r^{\alpha}_{il}(r^{\gamma}_{il} r^{\gamma'}_{il} - \tfrac{1}{3}\delta_{\gamma\gamma'}) + \tfrac{1}{2}(\delta_{\alpha\gamma} r^{\gamma'}_{il} + \delta_{\alpha\gamma'} r^{\gamma}_{il}) - r^{\gamma}_{il} r^{\gamma'}_{il} r^{\alpha}_{il} . \tag{A7}$$

From this equation can be easily seen that

$$F^{\gamma\gamma'}_{\alpha\beta}(i,i';l,l';t=0) = \hat{D}^{(1)}_{\alpha\gamma\gamma'} \hat{D}^{(2)}_{\beta\gamma\gamma'} Q^{ili'l'}(\vec{A}_1, \vec{A}_2) \mid_{\vec{A}_1 = \vec{A}_2 = \vec{0}} , \tag{A8}$$

where

$$\hat{D}^{(n)}_{\alpha\gamma\gamma'}=\xi\frac{\partial}{\partial A_n^\alpha}\left[\frac{\partial^2}{\partial A_n^\gamma\partial A_n^{\gamma'}}-\frac{1}{3}\delta_{\gamma\gamma'}\right]+\frac{1}{2}\left[\delta_{\alpha\gamma}\frac{\partial}{\partial A_n^{\gamma'}}+\delta_{\alpha\gamma'}\frac{\partial}{\partial A_n^\gamma}\right]-\frac{\partial^3}{\partial A_n^\gamma\partial A_n^{\gamma'}\partial A_n^\alpha},$$

and the function $Q^{ili'l'}(\vec{A}_1,\vec{A}_2)$ is defined as

$$Q^{ili'l'}(\vec{A}_1,\vec{A}_2)=\int d\vec{\Omega}_1 d\vec{\Omega}_2\Pi^{il}(\vec{\Omega}_2)\Pi^{ili'l'}(\vec{\Omega}_2,\vec{\Omega}_1)e^{A_1^x\sin\theta_1\cos\varphi_1+A_1^y\sin\theta_1\sin\varphi_1+A_1^z\cos\theta_1}e^{A_2^x\sin\theta_2\cos\varphi_2+A_2^y\sin\theta_2\sin\varphi_2+A_2^z\cos\theta_2}$$

$$=\int d\vec{R}_1 d\vec{R}_2 e^{\vec{A}_1\cdot\vec{R}_1}e^{\vec{A}_2\cdot\vec{R}_2}\Pi^{il}(\vec{R}_1)\Pi^{ili'l'}(\vec{R}_2,\vec{R}_1)\delta(|\vec{R}_1|^2-1)\delta(|\vec{R}_2|^2-1)\,. \tag{A9}$$

This procedure to calculate the configurational averages allows us to deduce some of their general properties directly from the properties of the probability distribution function used. Indeed, because of the invariance of scalar production under any point symmetry operation,[14] the symmetry group of $Q^{ili'l'}(\vec{A}_1,\vec{A}_2)$ must include all the symmetry operations of $\Pi^{il}(\vec{R})$. Therefore, recalling that $\partial/\partial A^\alpha$ and A^α have the same symmetry properties and that $\Pi^{il}(\vec{R})$ contains the cubic symmetry in our case, then relation (A4) follows directly from Eq. (A8). The factor $\Theta^{\gamma\gamma'}(\vec{k},j\,|\,\vec{q})$ defined in Eq. (A2) can be now rewritten using Eq. (A4), introducing the eigenvectors[15]

$$\vec{w}(\vec{k},j\,|\,i)=e^{-i\vec{k}\cdot\vec{x}_i}\vec{e}(\vec{k},j\,|\,i)\,,$$

and supposing that (this hypothesis will be justified later in the case of α-AgI)

$$F^{\gamma\gamma'}(i,i';l,l';t=0)=A_{ii'}^{\gamma\gamma'}\Theta(|\vec{x}_l-\vec{x}_{l'}+\vec{x}_i-\vec{x}_{i'}|)\,, \tag{A10}$$

we find

$$\Theta^{\gamma\gamma'}(\vec{k},j\,|\,\vec{q})=N\sum_l\sum_{i,i'}e^{-i(\vec{q}-\vec{k})\cdot(\vec{x}_l-\vec{x}_{l'}+\vec{x}_i-\vec{x}_{i'})}\frac{A_{ii'}^{\gamma\gamma'}}{\sqrt{M_iM_{i'}}}\vec{w}(\vec{k},j\,|\,i)\vec{w}(\vec{k},j\,|\,i')\Theta(|\vec{x}_l-\vec{x}_{l'}+\vec{x}_i-\vec{x}_{i'}|)\,. \tag{A11}$$

By replacing sums with integrals in (A11) we obtain

$$\Theta^{\gamma\gamma'}(\vec{k},j\,|\,\vec{q})=\frac{N}{\Omega}\left[\sum_{i,i'}\frac{A_{ii'}^{\gamma\gamma'}}{(M_iM_{i'})^{1/2}}\vec{w}(\vec{k},j\,|\,i)\vec{w}(\vec{k},j\,|\,i')\right]\int dr\,e^{-i(\vec{q}-\vec{k})\cdot\vec{r}}\Theta(|\vec{r}|)\,. \tag{A12}$$

In the case of α-AgI, $M_i=M$ with $i=1,2$, and if we denote, with $\tilde{\Theta}(|\vec{k}|)$, the Fourier transform of $\Theta(|\vec{r}|)$, Eq. (A12) becomes

$$\Theta^{\gamma\gamma'}(\vec{k},j\,|\,\vec{q})=\frac{N}{2M}\left[\sum_{i,i'}A_{ii'}^{\gamma\gamma'}\right]\tilde{\Theta}(|\vec{k}-\vec{q}|)\,. \tag{A13}$$

It is generally assumed[15] that the correlation function $\Theta(r)$ has a Gaussian shape $\Theta(r)=e^{-r^2/2\sigma^2}$ where σ is a "correlation length." The final expression for the scattering intensity is therefore

$$I_{\gamma\gamma'}(\omega)=A^{\gamma\gamma'}[n(\omega)+1]\times\sum_{\vec{k},j}\frac{1}{2\omega_j(\vec{k})}e^{-(\vec{q}-\vec{k})/2\bar{K}^2}\mathrm{Im}\,D_{\vec{k}j}(\omega)\,, \tag{A14}$$

where

$$A^{\gamma\gamma'}=\left[\frac{N}{2M}\frac{(2\pi)^{3/2}}{\Omega}\frac{1}{\bar{K}^3}\sum_{i,i'}A_{ii'}^{\gamma\gamma'}\right]$$

and

$$\bar{K}=\frac{1}{\sigma}\,.$$

Using now the description in terms of d-site cages in the expression of the polarizability derivatives [see Eq. (A7)], we are able to evaluate the correlation function $\tilde{F}^{\gamma\gamma'}(i,i';l,l';t=0)$ for some values of $l'-l$ in the case of C_3^0,C_5^0 configurations, for instance. In such a situation the bcc elementary cell $l\equiv(l_1,l_2,l_3)$ is assumed to be made up by pairs ($i=1,2$) of C_3^0,C_5^0 iodines; this means looking at the arrangement of the silver ions on a given cage as a characteristic of the iodine in its center.

For the lower values of $(l'-l)$ (i.e., for nearest- and next-nearest-neighbor cells) the evaluation of the configurational averages is now a simple tedious task, performed while looking for all the arrangements which can be compatible with a given arrangement belonging to the cell $l\equiv(0,0,0)$. In such a way the assumption (A10) may be verified and the order of magnitude of $\bar{K}=1/\sigma=0.25$ Å^{-1} is obtained by fitting the theoretical results with $\Theta(r)=e^{-r^2/2\sigma^2}$. Moreover, we note that in the case (C_3^0,C_5^0) we obtain

$$A_{ii'}^{\gamma\gamma'}=\begin{cases}n_i^2J^{\gamma\gamma'}, & i=i'\\ -n_1n_2\frac{1}{6}J^{\gamma\gamma'}, & i\neq i'\end{cases}$$

with $n_i=\{3,5\}$, where $J^{\gamma\gamma'}$ has been already evaluated in I. The negative value of the A term has the physical

meaning of an "antiferroelectric" arrangement of the microscopic fields due to the silver ions on the iodine 3-5 pairs which may contribute in lowering the electrostatic energy of such configurations.

APPENDIX B

We evaluate here the ratio intensity between an acoustical branch [$\omega(\vec{k})=c\,|\,\vec{k}\,|$] and an optical one with small $\vec{k}$ dispersion [i.e., $\omega(\vec{k})\simeq\omega_0=$const] in the harmonic approximation, where

$$\int d\omega\,\mathrm{Im}\,D_{\vec{k}j}(\omega)=\pi\ . \tag{B1}$$

From Eqs. (13) and (B1) we obtain for the jth branch,

$$\int d\omega\,J^{*}_{\gamma\gamma'}(\omega)=\pi J_{\gamma\gamma'}\sum_{\vec{k}} e^{-k^2/2\bar{K}^2}\frac{A}{\omega_j(\vec{k})}\ , \tag{B2}$$

where from (A7),

$$A=\frac{1}{\bar{K}^3}\frac{(2\pi)^{3/2}}{\Omega}\sum_{i,i'}A_{ii'}^{\gamma\gamma'}\ .$$

Replacing, in (B2),

$$\sum_{\vec{k}} e^{-k^2/2\bar{K}^2}/\omega_j(\vec{k})\rightarrow\frac{\Omega}{(2\pi)^3}(4\pi)\times\int_0^{\infty}k^2e^{-k^2/2\bar{K}^2}\frac{1}{\omega_j(\vec{k})}d\vec{k}\ ,$$

we have the two results

$$\int d\omega\,J^{\mathrm{acous}}_{\gamma\gamma'}(\omega)\simeq\pi J_{\gamma\gamma'}\frac{A}{c}\frac{\Omega}{(2\pi)^3}(4\pi)\bar{K}^2,\quad\omega(\vec{k})=c\,|\,\vec{k}\,| \tag{B3}$$

and

$$\int d\omega\,J^{\mathrm{opt}}_{\gamma\gamma'}(\omega)\simeq\pi J_{\gamma\gamma'}\frac{A}{\omega_0}\frac{\Omega}{(2\pi)^3}(4\pi)\sqrt{8\pi}\bar{K}^3,\quad\omega(\vec{k})=\omega_0\ . \tag{B4}$$

Then using the simplification

$$\langle\omega_0\rangle=\tfrac{1}{3}\sum_{j=1,3}\omega_{0j}$$

and introducing $\bar{\omega}_L=c_L\bar{K}$, we obtain, for Eq. (21),

$$\chi(T)\propto\bar{K}$$

and

$$\sum_{j=1}^{3}\int d\omega\,J^{\mathrm{opt}}_{\gamma\gamma'}(\omega)\Big/\int d\omega\,J^{\mathrm{LA}}_{\gamma\gamma'}(\omega)\simeq3.8\frac{\bar{\omega}_L}{\langle\omega_0\rangle}\simeq1\ ,$$

in agreement with the experimental value of $\simeq1.3$.

[1] A. Fontana, G. Mariotto, and M. P. Fontana, Phys. Rev. B 21, 1102 (1980).

[2] G. Mariotto, A. Fontana, E. Cazzanelli, F. Rocca, M. P. Fontana, V. Mazzacurati, and G. Signorelli, Phys. Rev. B 23, 4782 (1981).

[3] V. Mazzacurati, G. Ruocco, G. Signorelli, E. Cazzanelli, A. Fontana, and G. Mariotto, Phys. Rev. B 26, 2216 (1982).

[4] M. J. Delaney and S. Ushioda, Phys. Rev. B 16, 1410 (1977).

[5] G. Mariotto, A. Fontana, E. Cazzanelli, and M. P. Fontana, Phys. Status Solidi B 101, 391 (1981).

[6] R. Alben and G. Burns, Phys. Rev. B 16, 3746 (1977); G. Burns, F. H. Dacol, and R. Alben, Solid State Commun. 32, 71 (1979).

[7] W. Bührer, R. M. Nicklow, and P. Brüesch, Phys. Rev. B 17, 3362 (1978).

[8] G. Winterling, W. Seen, M. Grimsditch, and R. Katiyar, in *Proceedings of the International Conference on Lattice Dynamics,* edited by M. Balkanski (Flammarion, Paris, 1977), p. 553.

[9] R. J. Nemanich, R. M. Martin, and J. C. Mikkelsen, Jr., Solid State Commun. 32, 79 (1979).

[10] P. Brüesch, W. Bührer, and H. J. M. Smeets, Phys. Rev. B 22, 970 (1980).

[11] A. A. Maradudin, E. W. Montroll, E. W. Weiss, and I. Ipatova, in *Theory of Lattice Dynamics in the Harmonic Approximation,* Suppl. 3 of *Solid State Physics,* edited by H. Ehrenreich, F. Seitz, and D. Turnbull (Academic, New York, 1971).

[12] G. Winterling, Phys. Rev. B 12, 2432 (1975).

[13] P. A. Fleury, in Proceedings of the 2nd International Meeting on Ferroelectricity, Kyoto, 1969 [J. Phys. Soc. Jpn. Suppl. 28, (1970)], p. 167.

[14] A. A. Abrikosov, L. P. Gor'kov, and I. E. Dzyaloshinski, in *Methods of Quantum Field Theory in Statistical Physics,* edited by A. Silverman (Dover, New York, 1963).

[15] See, for example, J. H. Ziman, *Models of Disorder* (Cambridge University Press, Cambridge, England, 1979).